c-Jun N-terminal kinase mediates microtubule-depolymerizing agent-induced microtubule depolymerization and G2/M arrest in MCF-7 breast cancer cells

Juan Chen[a,b], Wei-Liang Sun[a], Bohdan Wasylyk[c], Yan-Ping Wang[a,b] and Hong Zheng[a,b]

Microtubule-binding agents (MBAs) form one of the most important anticancer-drug families, but their molecular mechanisms are poorly understood. MBAs such as paclitaxel (PTX) stabilize microtubules, whereas XRP44X (a novel pyrazole) and combretastatins A4 (CA4) destabilize microtubules. These two different types of MBAs have potent antitumor activity. Comparisons of their effects on signal transduction and cellular responses will help uncover the molecular mechanism by which MBAs affect tumor cells. We used MCF-7 cells to compare the effects of the three MBAs on the cytoskeleton, cell cycle distribution, and activation of the three major mitogen-activated protein kinase (MAPK) signaling cascades [extracellular signal-related kinases, c-Jun N-terminal kinase (JNK), and p38 MAPK] using pharmacological inhibitors. The G2/M phase arrest was induced following polymerization of microtubules by PTX and depolymerization by XRP44X and CA4. The three major MAPKs were rapidly activated by XRP44X, and extracellular signal-related kinases and p38 by PTX, whereas JNK did not quickly respond to PTX. Pharmacological inhibitors indicated that activation of JNK is principally required for XRP44X- and CA4-induced microtubule depolymerization and G2/M phase arrest. Our results suggest that early phosphorylation of JNK is a specific mechanism involved in microtubule depolymerization by certain MBAs.
***Anti-Cancer Drugs* 23:98–107 © 2011 Wolters Kluwer Health | Lippincott Williams & Wilkins.**

Anti-Cancer Drugs 2012, **23**:98–107

Keywords: breast cancer, G2/M arrest, JNK, microtubule-binding agents, microtubule depolymerization

[a]Laboratory of Tumor Molecular Diagnosis, [b]State Key Laboratory of Biotherapy, West China Hospital, West China Medical School, Sichuan University, Chengdu, People's Republic of China and [c]Institut de Génétique et de Biologie Moléculaire et Cellulaire, Centre National de la Recherche Scientifique, Institut National de la Sante et de la Recherche Medicale, Université Louis Pasteur, Illkirch, Cedex, France

Correspondence to Dr Hong Zheng, PhD, Laboratory of Tumor Molecular Diagnosis, West China Hospital, West China Medical School, Sichuan University, No. 37 Guo-xue-xiang, Chengdu, P.R. China
Tel: +86 28 8542 2973; fax: +86 28 8542 2685;
e-mail: hongzheng11@yahoo.com.cn

Juan Chen and Wei-Liang Sun contributed equally to this study.

Received 21 January 2011 **Revised** 7 August 2011
Revised form accepted 9 August 2011

Introduction

Microtubule-binding agents (MBAs) can be broadly classified on the basis of their effects on microtubule dynamics. Some MBAs stabilize microtubules and stimulate polymerization [e.g., paclitaxel (PTX) and epothilones/ixabepilone], whereas others destabilize microtubules and stimulate depolymerization (e.g., colchicine, vinca alkaloids, combretastatins, and CYT997). Both types of MBAs disrupt the tubulin–microtubule equilibrium, interfere with mitotic spindle formation, and induce cell cycle arrest, thereby causing apoptosis of cancer cells [1]. Despite the numerous studies of the ultimate effects of MBAs, the molecular mechanisms of their actions are still incompletely understood.

Microtubules consist of α-tubulin and β-tubulin heterodimers, and their dynamics are modulated by microtubule-associated proteins (MAPs) that bind to these subunits [2]. Mitogen-activated protein kinases (MAPKs) preferentially phosphorylate Ser/Thr-Pro motifs [3]. The abundance of such motifs on many MAPs suggests that MAPKs play critical roles in the phosphorylation of MAPs, thereby regulating microtubule behavior [4–7]. The MAPK superfamily has three major members in mammals: extracellular signal-related kinases (ERK1/2), c-Jun N-terminal kinase (JNK), and p38 MAPK. MBAs have various effects on MAPKs. In particular, prolonged treatment with vinblastine, vincristine, PTX, or colchicine leads to variable activation of JNK [8]. However, the rapid responses that follow MBA activation of MAPKs are different. For instance, in MCF-7 cultured breast cancer cells, 0.2 μmol/l PTX (polymerization stimulator) does not increase the activity of JNK within 2.5 h, whereas 0.2 μmol/l colchicine (depolymerization stimulator) significantly increases the activity of JNK [9].

XRP44X was originally identified as an efficient inhibitor of Ras-Erk-mediated phosphorylation of the ETS family transcription factor Net (Elk-3/SAP-2/Erp) [10]. Combretastatin A4 (CA4) and various analogues have antimitotic and vascular-disrupting effects, and are currently being evaluated in a number of clinical trials [11]. They depolymerize microtubules by binding to the

All supplementary digital content is available directly from the corresponding author.

0959-4973 © 2011 Wolters Kluwer Health | Lippincott Williams & Wilkins DOI: 10.1097/CAD.0b013e32834bc978

colchicine-binding site of β-tubulin. Normal microtubule dynamics are critical for cell proliferation, mitosis, motility, maintenance of cell shape, and signal transduction [12]. XRP44X-induced microtubule depolymerization leads to various abnormalities in vascular endothelial and human cancer cells with regard to growth, cell cycle progression, and aortal spouting, similar to CA4 [10]. However, the molecular mechanisms that mediate the effects of XRP44X and CA4 are not well established.

In this study, we investigated the effects of PTX, XRP44X, and CA4 on molecular signal transduction, microtubule dynamics, and cellular responses in MCF-7 human breast cancer cells. We describe important novel aspects of the mechanisms by which these MBAs induce cytotoxicity.

Methods

Cells and reagents

MCF-7 cells (ATCC) were propagated at 37°C under 5% CO_2 in RPIM1640 medium supplemented with 10% calf serum. XRP44X [dissolved in dimethyl sulfoxide (DMSO)] was a kind gift from Sanofi-Aventis (Vitry-sur-seine, France); PTX was from Bristol-Myers Squibb (Mayaqueu, Puerto Rico, USA); and CA4 was purchased from Sigma-Aldrich (St. Louis, Missouri, USA). Tetramethylrhodamine B isothiocyanate (TRITC)-conjugated phalloidin, 3-(4,5-dimethylthiazol-2-yl)-2,5-diphenyltetrazolium bromide (MTT)], and propidium iodide (PI) were from Sigma-Aldrich. PD98059 (ERK inhibitor) and SB203580 (p38 inhibitor) were from Promega (Madison, Wisconsin, USA); U0126 (an ERK inhibitor) and SP600125 (JNK inhibitor) were from Calbiochem (La Jolla, California, USA). bFGF was from PeproTech (London, UK). Anti-β-tubulin monoclonal, anti-diphosphorylated-ERK1/2 monoclonal, anti-ERK1/2 rabbit polyclonal, anti-phosphospecific-p38 monoclonal, anti-p38 monoclonal, anti-diphosphorylated-SAPK/JNK monoclonal, anti-SAPK/JNK rabbit polyclonal antibodies were from Cell Signaling Technology (Beverly, Massachusetts, USA).

Cell proliferation assay

A total of 1×10^4 cells were seeded in 96-well plates (BD Biosciences, San Jose, California, USA), allowed to attach overnight, and then exposed to the vehicle (1×10^{-6} v/v DMSO) alone, XRP44X, or PTX for 2 days to determine the IC_{50}, or for 0.5–5 days to monitor growth with time. IC_{50} and cell proliferation were assessed by a colorimetric assay using MTT (Sigma-Aldrich) as described previously [13]. Absorbance in each well was measured at 490 nm using a Multiskan Spectrum (Thermo Life Science France S.A., Cergy Pontoise, France).

Flow cytometry

Cells were pretreated with or without inhibitors, exposed to agents for different times in growth medium, collected in 0.125% trypsin, washed twice in PBS, and fixed in 70% methanol overnight at −20°C. Then, the cells were resuspended in PBS with 50 μg/ml PI and 10 μg/ml RNase A (Tiangen, Beijing, China) at 4°C for 30 min. Flow cytometry data were analyzed with the Cytomics FC500 (Beckman Coulter Ltd, Miami, Florida, USA).

Immunofluorescence microscopy

Cells were cultured on coverslips for 24–48 h before treatment, pretreated with or without inhibitors, and then exposed to the compounds. For microtubule staining, cells were fixed in 3.75% formaldehyde in PBS for 10 min, permeabilized with 0.1% Triton X-100 for 5 min, blocked in 5% normal goat serum for 1 h at 37°C, incubated with anti-β-tubulin antibody overnight at 4°C, and then fluorescein isothiocyanate-conjugated goat anti-rabbit secondary antibody for 1 h at room temperature. For F-actin staining, fixed cells were blocked in 1% BSA, and then incubated with 5 U/ml TRITC-conjugated phalloidin for 20 min. 4′,6-Diamidino-2-phenylindole (DAPI) was used for nuclear staining. Fluorescence images were taken with a Nikon Eclipse TE200 microscope and processed with Adobe Photoshop software.

Assessment of cellular microtubule sensitivity [14] to agent-mediated microtubule disruption

When cells are rapidly lysed using Pipes-EGTA-based buffers with detergents, assembled cytoplasmic microtubules remain preserved in their polymerized state and are detergent-insoluble [15]. This differential extraction procedure, which separates detergent-soluble and detergent-insoluble tubulin, was used to assess the sensitivity of MCF-7 microtubules to agent-mediated disruption. Cells were extracted for 5 min at 37°C in Pipes-EGTA-based lysis buffer (80 mmol/l Pipes-KOH, pH 6.8, 1 mmo/l $MgCl_2$, 1 mmol/l EGTA, 0.2% TritonX-100, 10% glycerol) with a protease inhibitor cocktail (100 μg/ml phenylmethanesulfonyl fluoride, 2 μg/ml aprotinin, 2 μg/ml leupeptin, and 1 μg/ml pepstatin), as described previously [16]. Supernatants containing detergent-soluble tubulin were transferred to new tubes, and detergent-insoluble polymerized tubulin in the precipitates was extracted with lysis buffer A [50 mmol/l Tris (pH 8.8), 150 mmol/l NaCl, 1% NP40, 0.1% SDS, 5 mmol/l EDTA, 0.25% sodium deoxycholate (pH 10.0), 20 mmol/l NaF] with the same protease inhibitor cocktail, and then analyzed by western blotting for β-tubulin.

Western blotting

For analysis of the MAPK activity, the treated cells were harvested in lysis buffer A with the protease inhibitor cocktail. For analysis of microtubule sensitivity to agent-mediated disruption, differential extracts, comprised of detergent-soluble and detergent-insoluble fractions from treated cells, were processed as described above. Samples containing equal amounts of protein were fractionated by 12% SDS-PAGE and transferred to a polyvinylidene fluoride membranes (Roche, Mannheim, Germany) using the Bio-Rad microassay system (Bio-Rad, Hemel

Hempstead, UK). Immunoreactive bands were visualized by enhanced chemiluminescence (Pierce, Rockford, Illinois, USA). Densitometric analysis of the film was performed using a HP LaserJet 3055 scanner and Bio-Rad Discovery software (Quantity One) (Bio-Rad).

Statistical analysis

All numerical data were expressed as mean ± SD. Data were analyzed by the independent-samples *t*-test using SPSS software. All tests were two-sided. A *P*-value less than 0.05 was considered significant.

Results

XRP44X and PTX inhibit MCF-7 cell proliferation

The effects of XRP44X and PTX on the growth and proliferation of MCF-7 cells were compared using the MTT assay. Cells were cultured with vehicle (1×10^{-6} v/v DMSO), XRP44X, or PTX for 2 days to determine the IC_{50}, or for 0.5–5 days to analyze the time course of growth. Compared with the vehicle (set to 100%), cell growth was inhibited at XRP44X concentrations of 5 nmol/l ($P < 0.001$) and above, and PTX concentrations of 1.17 nmol/l (1.17 nmol/l = 1.00 ng/ml) ($P = 0.022$) and above (Fig. 1a). The IC_{50} of XRP44X and PTX were 22.6 (± 2.6) nmol/l and 24.0 (± 3.5) nmol/l (calculated by a curve-fitting algorithm), respectively. At concentrations of 100 nmol/l for XRP44X and 117 nmol/l for PTX, the growth curves of the cells almost overlapped (Fig. 1b). Therefore, these concentrations were used for most subsequent experiments. DMSO alone did not affect MCF-7 cell proliferation (data not shown).

Fig. 1

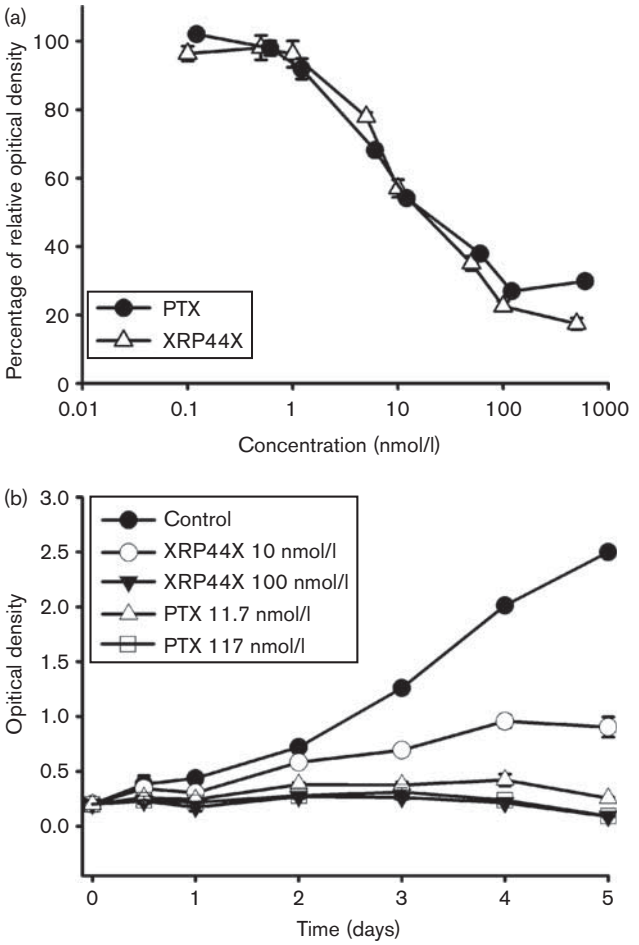

XRP44X and PTX (paclitaxel) inhibit proliferation of MCF-7 cells. (a) Effects of XRP44X and PTX on growth of MCF-7 cells. Cells were treated for 48 h with the indicated concentrations of XRP44X or PTX, and cell growth was assessed using the MTT assay. Growth inhibition is shown as a percentage of control (1×10^{-6} v/v DMSO) cells. (b) Growth curves of MCF-7 cells treated with XRP44X or PTX, as determined by the MTT assay. Cells were cultured with or without the indicated concentrations of XRP44X or PTX for 0.5–5 days (for PTX, 1.17 nmol/l = 1.00 ng/ml). The results presented were from one representative of three experiments. DMSO, dimethyl sulfoxide; MTT, 3-(4,5-dimethylthiazol-2-yl)-2,5-diphenyltetrazolium bromide; PTX, paclitaxel.

XRP44X and PTX induce accumulation of cells in the G2/M phase

XRP44X arrests endothelial cells in the G2/M phase [10]. We therefore analyzed the effect of XRP44X on the cell cycle of MCF-7. As shown in Fig. 2a, XRP44X increased the percentage of MCF-7 cells in the G2/M phase at 6 h ($P = 0.002$); the majority of cells were in the G2/M phase at 12 h ($P < 0.001$), and nearly 80% of the cells were in the G2/M phase after 24 h ($P < 0.001$). PTX had similar effects (Fig. 2b). PTX induced significant apoptosis ($P = 0.027$) after 24 h, whereas XRP44X did not (Supplementary Fig. 1). Another microtubule-depolymerizing agent, CA4, also had little effect on apoptosis at this time point, in contrast with PTX (Supplementary Fig. 1).

XRP44X depolymerizes, but PTX polymerizes microtubule

We used indirect immunofluorescence to examine the effects of XRP44X and PTX on the microtubules of MCF-7 cells. As shown in Fig. 2c, 100 nmol/l of XRP44X led to depolymerization of microtubules, resulting in granular staining in the cytoplasm, whereas PTX induced the formation of microtubule bundles. Furthermore, we compared the effects of XRP44X and PTX on filamentous actin (F-actin) by staining with TRITC-conjugated phalloidine. As shown in Fig. 2d, neither agent had any effect on the actin cytoskeleton morphology.

To confirm these results on microubules, differential extraction was performed to separate cytoskeletal detergent-insoluble polymerized (P) or detergent-soluble (S) depolymerized fractions, and followed by western blotting. As shown in Fig. 2e, 100 nmol/l XRP44X led to very significant depolymerization of microtubules, as indicated by the decrease in polymerized (P) and increase in soluble (S) tubulin. In contrast, PTX treatment led to nearly complete tubulin polymerization. Densitometric analysis of these results (Fig. 2f) indicated that the

Fig. 2

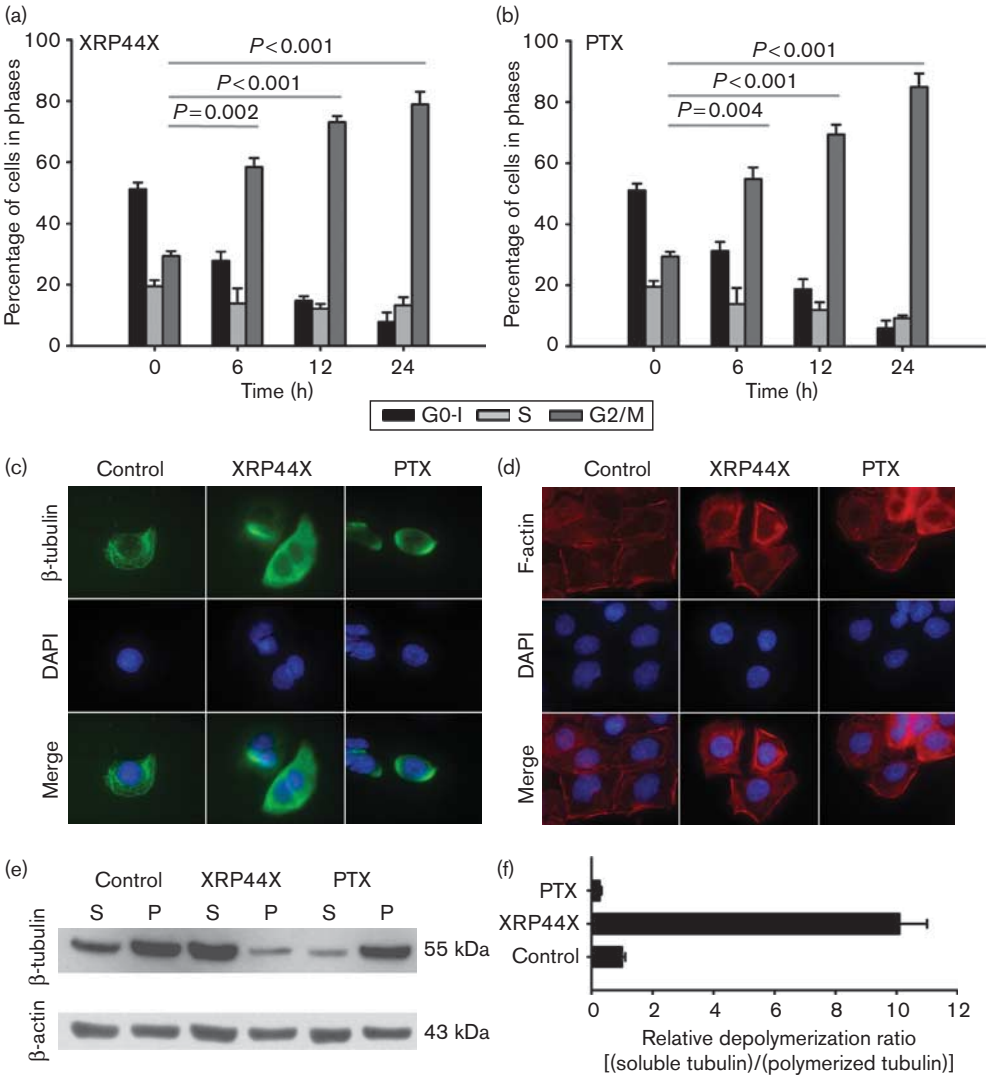

XRP44X and PTX induce G2/M phase arrest, but have different effects on microtubules. Effects of XRP44X (a) and PTX (b) on MCF-7 cell cycle distribution. Cells were treated with the vehicle (1×10^{-6} v/v DMSO), XRP44X (100 nmol/l), or PTX (117 nmol/l) for the indicated times, then washed and resuspended in PBS with PI (5 mg/ml). DNA ploidy was analyzed by flow cytometry. *P* values indicate the significance between G2/M phases. The results presented are the mean ± SD of three individual experiments. (c and d) XRP44X induces depolymerization of microtubules and PTX induces polymerization, whereas neither agent affects actin morphology. MCF-7 cells were plated on coverslips for 24–48 h and exposed to the vehicle (1×10^{-6} v/v DMSO), XRP44X (100 nmol/l), or PTX (117 nmol/l) for 90 min. Tubulin (c) was stained with an anti-β-tubulin antibody followed by FITC-conjugated secondary antibody, and F-actin (d) with TRITC-conjugated phalloidin (see Methods). Cells were examined by fluorescence microscopy (×1000). DAPI (blue) stains nuclei. Representative fields are shown. (e) Western blotting analysis of soluble (S) and polymeric (P) tubulin fractions. Cells were treated with vehicle (1×10^{-6} v/v DMSO), XRP44X (100 nmol/l), or PTX (117 nmol/l) for 90 min, and equal amounts of protein were loaded. The results presented are from one representative of three experiments. β-Actin was used as the loading control. (f) Quantitative analysis of (e) showed that the ratio between soluble and polymeric tubulin fractions reached approximately 10 : 1 with XRP44X treatment, but only approximately 1 : 4 with PTX. The results presented are the mean ± SD of three individual experiments. DAPI, 4′,6-diamidino-2-phenylindole; DMSO, dimethyl sulfoxide; FITC, fluorescein isothiocyanate; PTX, paclitaxel.

relative depolymerization ratio [(soluble tubulin)/(polymerized tubulin)] following XRP44X treatment was 10-fold greater than the control ($P = 0.003$).

XRP44X and PTX affect the phosphorylation states of MAPKs

To investigate the effects of XRP44X and PTX on the stimulation of ERK, p38 MAPK, and JNK, antibodies against the activated form of these MAPKs were used. Our results showed that treatment of MCF-7 cells with XRP44X led to the activation of all three MAPKs, but with different kinetics (Fig. 3a). XRP44X activated ERK within 7.5 min and started to decline by 45–60 min, but the level remained above basal at 120 min. p38 MAPK peaked more sharply around 15 min. JNK was activated more slowly, being detectable around 30 min and continuing to increase for at least 120 min.

Fig. 3

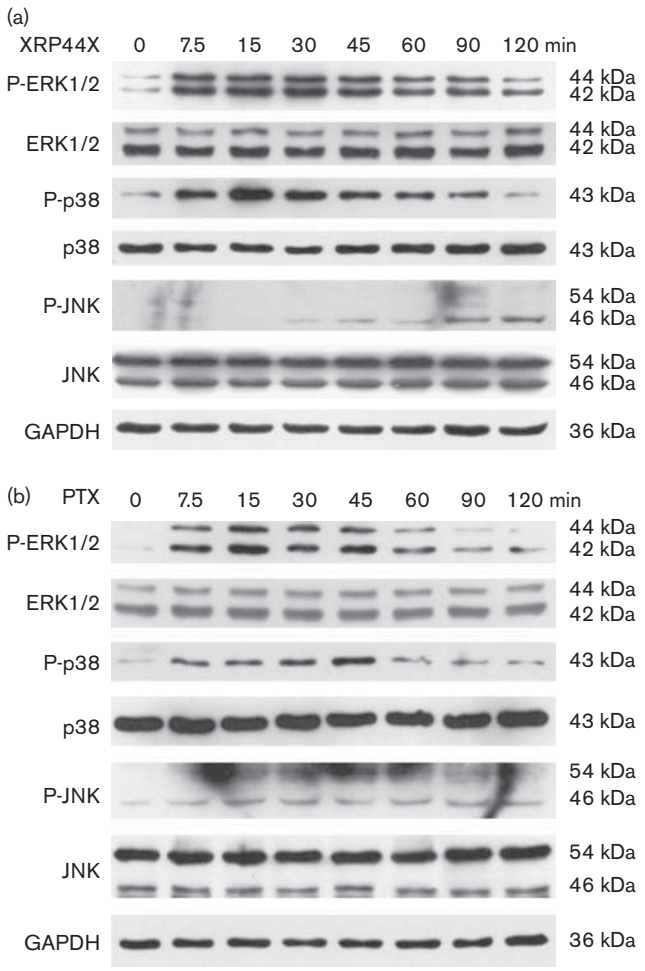

Effects of XRP44X or PTX on the phosphorylation of ERK (p42/p44), p38, and JNK (p46/p54). MCF-7 cells were treated with 100 nmol/l XRP44X (a) or 117 nmol/l PTX (b) for the indicated times. Phosphorylated and total proteins were detected with specific antibodies. The results presented were from one representative of three experiments. GAPDH was used as a loading control. ERK, extracellular signal-related kinases; JNK, c-Jun N-terminal kinase; PTX, paclitaxel.

The effect of PTX on MAPK activation was different from that of XRP44X (Fig. 3b). It stimulated ERK activity, with a more distinct peak at 15 min, and there was a notable reduction at 60 min. Activation of p38 MAPK was slower, with a peak at 45 min, and activity decreased thereafter. Interestingly, PTX had no detectable effect on JNK activity, in agreement with previous studies [17,18]. We also investigated the dose dependency of activation of JNK by XRP44X and PTX after 45 min of treatment. Around 50–1000 nmol/l XRP44X induced JNK activity, whereas 1.17–1170 nmol/l PTX had no effect (Supplementary Fig. 2).

A previous study showed that XRP44X inhibited bFGF-stimulated phosphorylation of ERK1/2 in HUVEC [10]. We found that XRP44X could also induce phosphorylation of ERK, which seemed to contradict this finding. In the previous work, HUVEC cells were pretreated with XRP44X before adding bFGF. Using a similar protocol with MCF-7, we also found that XRP44X pretreatment inhibited bFGF activation of ERK (Supplementary Fig. 3a), with the maximal effect at 500 nmol/l (Supplementary Fig. 3b). Our results indicate that XRP44X-treated cells are refractory to bFGF treatment. The mechanisms of this effect are an interesting subject for further study.

Inhibition of JNK, but not ERK and p38, blocks the effects of XRP44X

Specific inhibitors of ERK, p38 MAPK, and JNK were used to determine whether XRP44X-mediated alterations of microtubule dynamics and cell cycle distribution were due to activation of these MAPKs. Cells were pretreated with the selective inhibitors for 1 h, and then with XRP44X. As indicated by β-tubulin indirect immunofluorescence, only the JNK inhibitor affected XRP44X-induced microtubule depolymerization (Fig. 4a–d; PD98059 yielded results similar to U0126; data not shown), whereas treatment with the JNK inhibitor alone had no obvious effect (Fig. 4a and b).

Western blotting of the soluble and polymerized forms of β-tubulin also showed that XRP44X-induced depolymerization was reduced in the presence of the JNK inhibitor SP600125, but not the p38 and ERK inhibitors (Fig. 5a). Quantification of the western-blotting experiments showed that treatment with SP600125 and XRP44X decreased the soluble/polymerized tubulin ratio from approximately 10 : 1 to approximately 4 : 1 ($P < 0.001$) (Fig. 5b). Treatment of cells with the ERK inhibitor, the p38 inhibitor, or combinations of each inhibitor with XRP44X did not alter the ratio of soluble to polymerized forms of tubulin (Fig. 5b). These results indicate that activation of JNK, but not ERK or p38, is necessary for the induction of microtubule depolymerization by XRP44X.

As shown in Fig. 4, inhibitors of JNK, ERK, and p38 MAPK had no effect on the morphology of PTX-induced microtubule polymerization. Western blotting following treatment with the JNK inhibitor showed that there is no difference between treatment with PTX alone and treatment with PTX and SP600125 (Fig. 5a and b). These results show that although PTX induces rapid formation of microtubule bundles, this effect is not dependent on JNK activity.

The regulation of microtubule polymerization and depolymerization is critical for the modulation of mitosis. Thus, to further investigate the role of JNK in XRP44X-stimulated and PTX-stimulated cell cycle arrest, we treated MCF-7 cells with SP600125 before the addition of agents. As shown in Fig. 5c and d, SP600125 attenuated G2/M arrest markedly following 12 h of treatment with XRP44X ($P = 0.006$), but this effect did

Fig. 4

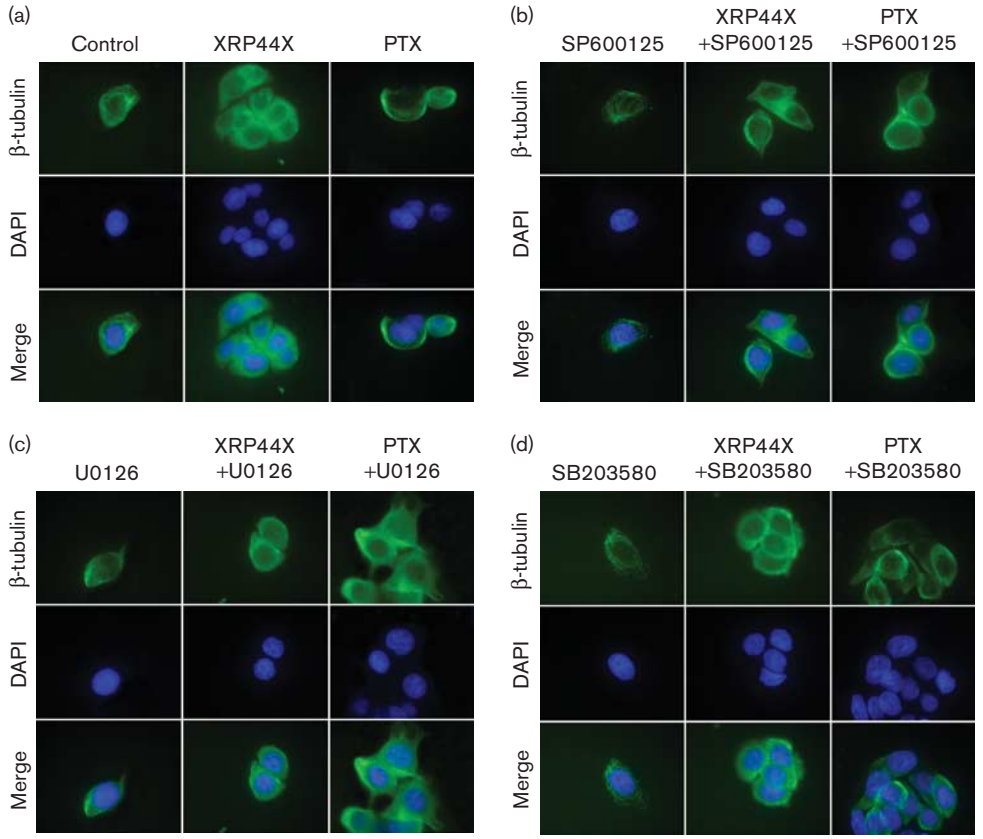

Effects of MAPK inhibitors on XRP44X-induced or PTX-induced microtubule morphological changes. Inhibition of JNK, but not ERK/p38, abrogates XRP44X-induced microtubule depolymerization. MCF-7 cells were plated on coverslips for 24–48 h, pretreated with vehicle [1×10^{-6} v/v DMSO (a)], SP600125 [25 μmol/l (b)], U0126 [2.5 μmol/l, (c)], PD98059 (25 μmol/l, data not shown), SB203580 [25 μmol/l (d)] for 1 h, and then exposed to 1×10^{-6} v/v DMSO, XRP44X (100 nmol/l), or PTX (117 nmol/l) for 90 min. Tubulin was stained with anti-β-tubulin antibody and FITC-conjugated secondary antibody, and cells were examined by fluorescence microscopy at ×1000. DAPI (blue) staining indicates nuclei. Representative fields are shown. DAPI, 4′,6-diamidino-2-phenylindole; DMSO, dimethyl sulfoxide; ERK, extracellular signal-related kinases; FITC, fluorescein isothiocyanate; JNK, c-Jun N-terminal kinase; MAPK, mitogen-activated protein kinase; PTX, paclitaxel.

not occur in cells treated with SP600125 alone at the same time point. These results indicate that JNK activation is critical for XRP44X-induced G2/M phase arrest, and inhibition of JNK activity allows cells to enter the G1 phase. SP600125 also affected PTX-caused G2/M arrest, in a relatively weaker but significant manner (Fig. 5c and d) ($P = 0.027$).

CA4-elicited microtubule depolymerizing also depends on activation of JNK

To examine the generality of the role of JNK activation in the effects of microtubule-depolymerizing agents, we studied CA4. As expected, CA4 induced microtubule depolymerization (Fig. 6a, CA4). The JNK inhibitor SP600125 prevented CA4-induced depolymerization, as shown by the restoration of both normal morphology (Fig. 6a) and the ratio of the soluble and polymerized forms of β-tubulin (Fig. 6b). Cell cycle arrest in the G2/M phase by CA4 was largely counteracted by SP600125 (Fig. 6c). We also found that SP600125 partially abrogated the inhibition of MCF-7 cell proliferation by XRP44X and CA4, but not PTX (data not shown). Taken together, our results indicate that XRP44X and CA4 induce microtubule depolymerization, G2/M arrest, and inhibition of cell growth because of activation of JNK.

Discussion

Previous research has shown that XRP44X inhibits bFGF-stimulated ERK activation in HUVEC [10], indicating its potential to suppress tumor angiogenesis. Here, we investigated the antitumor effects and mechanism of XRP44X in human breast cancer cells (MCF-7), compared with PTX and CA4. Immunofluorescence and western-blotting analyses revealed that XRP44X and CA4 disrupted microtubules rapidly and reduced the amount of polymerized microtubules in MCF-7 cells. PTX, a well-known antimitotic drug that is approved for treatment of breast, ovarian, lung, head, and neck cancers, had the opposite effect on microtubules. Despite

Fig. 5

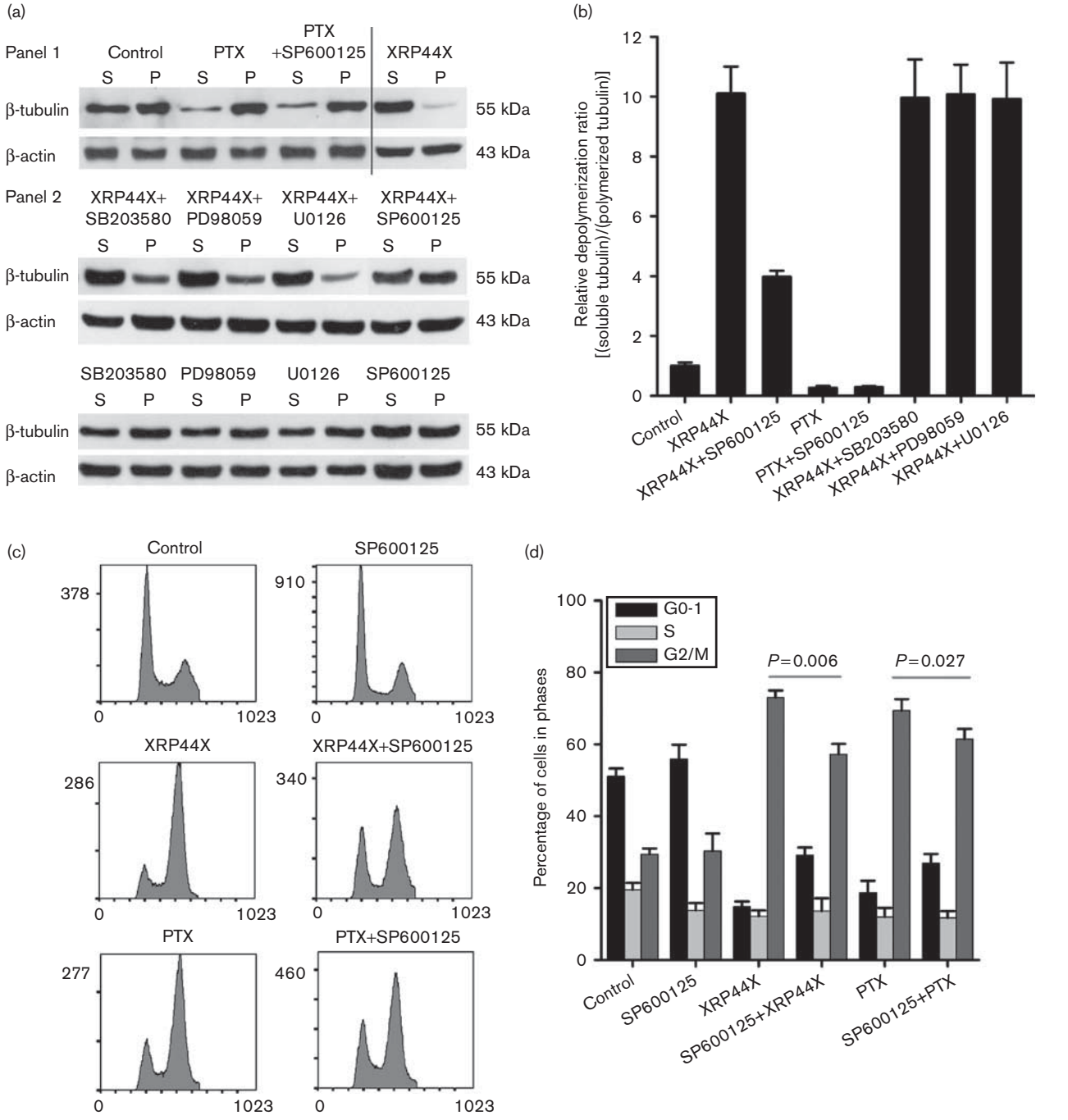

JNK is involved in XRP44X-induced microtubule depolymerization and G2/M phase arrest. (a and b) Western-blotting analysis of soluble (S) and polymeric (P) tubulin fractions. (a) Cells were incubated with or without MAPK inhibitors (25 μmol/l SB203580, 25 μmol/l PD98059, 2.5 μmol/l U0126, and 25 μmol/l SP600125) for 1 h, then exposed to vehicle (1×10^{-6} v/v DMSO), XRP44X (100 nmol/l), or PTX (117 nmol/l) for 90 min. Equal amounts of protein were loaded. 'Panel 1' shows that XPR44X stimulates microtubule depolymerization (soluble form of tubulin became the dominated form), whereas PTX induces polymerization (the polymerized form of tubulin became the dominated form). 'Panel 2' shows that the JNK inhibitor abolishes XRP44X-induced microtubule depolymerization, but not the ERK or p38 inhibitors. Meanwhile, the JNK inhibitor did not affect the effect of PTX on microtubules. (b) Quantitative analysis of (a) showed that the ratio between the soluble and the polymeric tubulin fractions reached approximately 10 : 1 in XRP44X treatment, whereas only approximately 4 : 1 in SP600125+XRP44X treatment. The results presented were mean ± SD of three individual experiments. (c and d) DNA ploidy analyses, as determined by PI staining. Cells were pretreated with or without SP600125, exposed to the vehicle (1×10^{-6} v/v DMSO), XRP44X (100 nmol/l), or PTX (117 nmol/l) for 12 h, then washed and resuspended in PBS with PI (5 mg/ml). DNA ploidy was determined by flow cytometry. The results presented in (d) are mean ± SD of three individual experiments. *P* values indicated the significance between G2/M phase. DMSO, dimethyl sulfoxide; ERK, extracellular signal-related kinases; JNK, c-Jun N-terminal kinase; MAPK, mitogen-activated protein kinase; PI, propidium iodide; PTX, paclitaxel.

Fig. 6

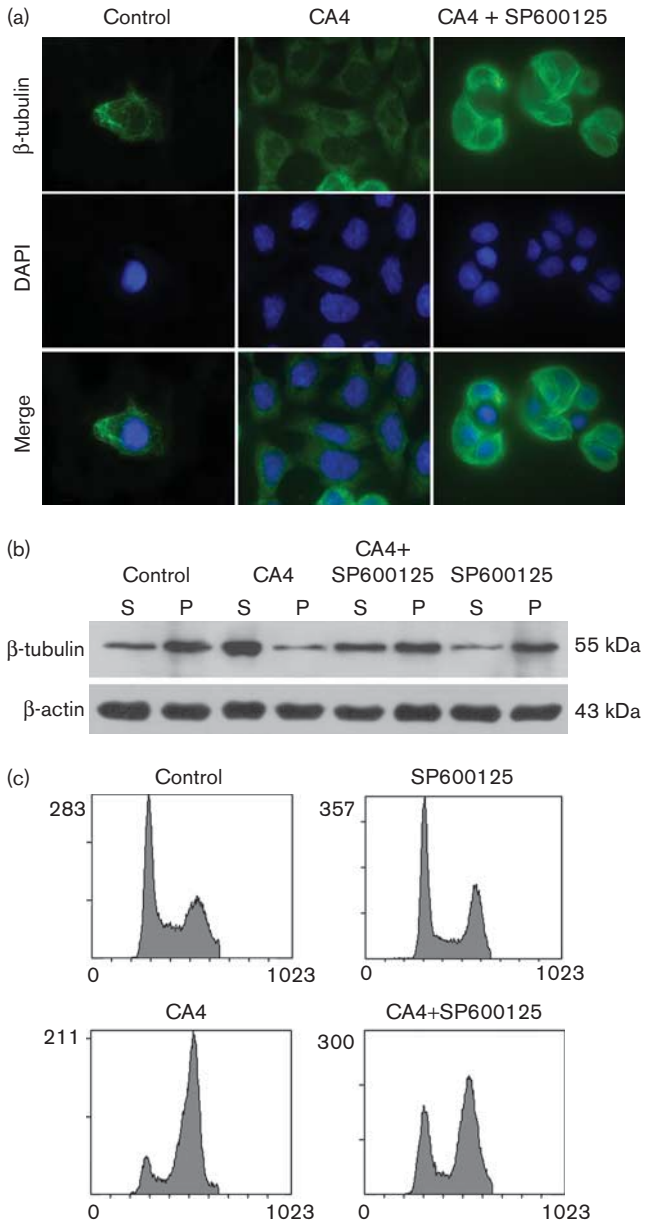

JNK is involved in CA4-induced microtubule depolymerization and G2/M phase arrest. (a) Effect of the JNK inhibitor on CA4-induced microtubule morphological changes. MCF-7 cells were plated on coverslips for 24–48 h, pretreated with or without SP600125 (25 μmol/l) for 1 h, and then exposed to the vehicle (5×10^{-4} v/v methanol) or CA4 (100 nmol/l) for 90 min. Tubulin was stained with anti-β-tubulin antibody and FITC-conjugated secondary antibody. Cells were examined by fluorescence microscopy at ×1000. DAPI (blue) staining indicates nuclei. (b) Western-blotting analysis of soluble (S) and polymeric (P) tubulin fractions. Cells were treated with either the vehicle (5×10^{-4} methanol) or CA4 (100 nmol/l) for 90 min, and equal amounts of protein were loaded. β-Actin was used as a loading control. (c) DNA ploidy analysis, as determined by PI staining. Cells were pretreated with or without SP600125, exposed to the vehicle (5×10^{-4} methanol) or CA4 (100 nmol/l) for 12 h, then washed and resuspended in PBS with PI (5 mg/ml). DNA ploidy was determined by flow cytometry. The results presented were from one representative of three experiments. CA4, combretastatins A4; DAPI, 4′,6-diamidino-2-phenylindole; FITC, fluorescein isothiocyanate; JNK, c-Jun N-terminal kinase; PI, propidium iodide.

their different effects on microtubules, these agents had similar antiproliferative effects on MCF-7 cells, with nearly equivalent IC_{50} values (data not shown for CA4).

Regulation of microtubule dynamics is critical, particularly during mitosis [19]. MBAs bind to tubulin subunits and interfere with the properties of microtubules. They prevent normal alignment of chromosomes, triggering the mitotic checkpoint [20], followed by apoptosis [21–23]. We found that XRP44X and CA4 treatment of MCF-7 cells led to accumulation in the G2/M phase with a time course that is similar to PTX. MBAs can have different effects during the cell cycle. They arrest cells in mitosis at the spindle checkpoint. In addition, microtubule disassembly has been shown to delay the G2/M transition at the morphogenesis checkpoint [24]. In contrast, agents that cause DNA damage can arrest cells in the G2 phase (premitosis). The technique we used (cell cycle distribution by DNA content) measures accumulation in the G2/M phase, and does not distinguish between different checkpoints. We have used the generic term G2/M arrest to take these possibilities into account. MBAs also induce apoptosis. We found that XRP44X and CA4 induce apoptosis of MCF-7 cells, but with slower kinetics than PTX (Supplementary Fig. 1). However, because the effects of PTX and XRP44X/CA4 on microtubules are distinct, the mechanisms by which they affect cell proliferation and ultimately cell fate may also be different.

Several studies have demonstrated that JNK modulates microtubules under normal physiological conditions. For example, JNK activation plays an essential role in neuron microtubule formation, growth, and normal microtubule dynamics, which are required for various neuron functions (e.g. maintenance of cell morphology and migration) [25–29]. However, under pathological conditions, JNK activation seems to be associated with abnormal microtubule behavior, such as microtubule disruption through phosphorylation of MAPs, e.g., kinesin-1 [30,31] and tau [32,33]. Preceding studies have established that tau has a role in breast cancer in response to MBAs [34]. Thus, it would be intriguing to examine the effects of XRP44X and CA4 on tau in breast cancer cells.

Teraishi *et al.* [35] observed that the thiazolidin compound DBPT caused JNK-dependent microtubule disruption in the human colon cancer cell line DLD-1. We also found that microtubule-depolymerizing agents XRP44X and CA4 destroy the microtubule cytoskeleton within 90 min because of rapid activation of JNK. However, microtubule polymerization by PTX was not affected by inhibition of JNK, ERK, or p38. Thus, our results suggest that rapid activation of JNK and regulation of the tubulin–microtubule equilibrium is a property of microtubule-depolymerizing agents, which distinguishes them from microtubule-polymerizing agents. Moreover, because it is a rapid and early event, microtubule depolymerization by JNK activation

appears to be a primary process in microtubule-depolymerizing agent-induced cellular responses.

We found that inhibition of JNK activity reversed XRP44X-induced and CA4-induced G2/M arrest partially. This partial effect may be related to the presence of other factors that regulate the cell cycle checkpoint, such as the cyclin-dependent kinase inhibitor p21waf1/cip1, whose expression was significantly elevated by XRP44X at the mRNA level (Supplementary Fig. 4). In addition, the inhibition of JNK activity by SP600125 might be incomplete; this leakage might contribute to the partial reversal of G2/M arrest. We observed that inhibition of JNK also attenuated PTX-induced G2/M phase accumulation weakly. The small effect of SP600125 on PTX-induced G2/M phase arrest suggests that it could be indirect. There might be other JNK-related mechanisms, besides JNK-induced microtubule depolymerization, that are involved in the effects of PTX on the cell cycle progression, but that are secondary to the major event. In our study, the abrogation of microtubule depolymerization by JNK inhibition was followed by the reversal of G2/M arrest. Therefore, we hypothesize that the induction of JNK activity by microtubule-depolymerizing agents, such as XRP44X and CA4, modulates microtubule formation and cell cycle checkpoints to prevent cell division in MCF-7. The functional significance of the different effects of the JNK inhibitor on cell cycle (G2/M) arrest in PTX-treated cells in relation to XRP44X-treated and CA4-treated cells needs to be further investigated to establish its functional significance.

Interestingly, other studies have shown that JNK activation plays crucial roles in growth arrest and apoptosis induced by either a novel antitumor agent Aplidin [36] or Tamoxifen [37] (through estrogen receptor-independent mechanism) in the ER-negative breast cancer cell line MBA-MB-231. Our results, when combined with the above findings, suggest that activation of JNK might be an important characteristic that could be used to classify antitumor agents.

The morphology of the actin cytoskeleton was not affected by XRP44X treatment in MCF-7, whereas it did have an effect in HUVEC. This difference suggests that the effects of XRP44X on the actin cytoskeleton may be cell type specific. Another interesting finding is that XRP44X activates ERK, but also antagonizes ERK activation induced by bFGF in our and other cell systems. FGFs stimulate various intracellular signal pathways and have diverse roles in cell biology, development, and physiology [38]. This antagonistic effect is seen after pretreatment of cells with XRP44X. XRP44X activates ERK initially (7.5–90 min); however, later (110 min) the level of activation decreases but still remains higher than baseline (Supplementary Fig. 3a, lanes 1 and 5, or inferred from Fig. 3a). At later time points, ERK activation by bFGF is inhibited compared with cells that have not been treated with XRP44X. This apparent paradox that XRP44X can both activate ERK and inhibit ERK activation raises questions about the mechanisms, and is an interesting question for further study.

Conclusion

We studied the signaling cascades and cellular responses that are induced by two different types of MBAs in a breast cancer cell line. The results show that XRP44X and CA4 induce microtubule depolymerization and cell cycle G2/M phase arrest through early JNK activation, whereas PTX induces polymerization and G2/M phase arrest without rapid activation of JNK. Combined with previous findings, these results indicate that activation of JNK could be used to classify and to distinguish the physiological effects of MBAs.

Acknowledgements

We thank Jie Zhang for the technical assistance with immunofluorescence microscopy, Yu Wang for assistance with western blotting, and Yun Zhao for help with the determination of p21waf1 mRNA expression.

Grant support: This study was supported by grants from the Science & Technology Department of Sichuan Province, China (No. 2008SZ0020), and the Ligue contre le cancer CCIR-GE.

Conflicts of interest

There are no conflicts of interest.

References

1 Jordan MA, Wilson L. Microtubules as a target for anticancer drugs. *Nat Rev Cancer* 2004; **4**:253–265.
2 Amos LA, Schlieper D. Microtubules and maps. *Adv Protein Chem* 2005; **71**:257–298.
3 Cobb MH, Goldsmith EJ. How MAP kinases are regulated. *J Biol Chem* 1995; **270**:14843–14846.
4 Sturgill TW, Ray LB. Muscle proteins related to microtubule associated protein-2 are substrates for an insulin-stimulatable kinase. *Biochem Biophys Res Commun* 1986; **134**:565–571.
5 Ray LB, Sturgill TW. Rapid stimulation by insulin of a serine/threonine kinase in 3T3-L1 adipocytes that phosphorylates microtubule-associated protein 2 in vitro. *Proc Natl Acad Sci USA* 1987; **84**:1502–1506.
6 Bogoyevitch MA, Kobe B. Uses for JNK: the many and varied substrates of the c-Jun N-terminal kinases. *Microbiol Mol Biol Rev* 2006; **70**:1061–1095.
7 Hu JY, Chu ZG, Han J, Dang YM, Yan H, Zhang Q, *et al*. The p38/MAPK pathway regulates microtubule polymerization through phosphorylation of MAP4 and Op18 in hypoxic cells. *Cell Mol Life Sci* 2010; **67**:321–333.
8 Stone AA, Chambers TC. Microtubule inhibitors elicit differential effects on MAP kinase (JNK, ERK, and p38) signaling pathways in human KB-3 carcinoma cells. *Exp Cell Res* 2000; **254**:110–119.
9 Shtil AA, Mandlekar S, Yu R, Walter RJ, Hagen K, Tan TH, *et al*. Differential regulation of mitogen-activated protein kinases by microtubule-binding agents in human breast cancer cells. *Oncogene* 1999; **18**:377–384.
10 Wasylyk C, Zheng H, Castell C, Debussche L, Multon MC, Wasylyk B. Inhibition of the Ras-Net (Elk-3) pathway by a novel pyrazole that affects microtubules. *Cancer Res* 2008; **68**:1275–1283.
11 Nagaiah G, Remick SC. Combretastatin A4 phosphate: a novel vascular disrupting agent. *Future Oncol* 2010; **6**:1219–1228.
12 Olmsted JB, Borisy GG. Microtubules. *Annu Rev Biochem* 1973; **42**: 507–540.
13 Vistica DT, Skehan P, Scudiero D, Monks A, Pittman A, Boyd MR. Tetrazolium-based assays for cellular viability: a critical examination of

selected parameters affecting formazan production. *Cancer Res* 1991; **51**:2515–2520.
14 Kanthou C, Tozer GM. The tumor vascular targeting agent combretastatin A-4-phosphate induces reorganization of the actin cytoskeleton and early membrane blebbing in human endothelial cells. *Blood* 2002; **99**: 2060–2069.
15 Bershadsky AD, Gelfand VI, Svitkina TM, Tint IS. Microtubules in mouse embryo fibroblasts extracted with Triton X-100. *Cell Biol Int Rep* 1978; **2**:425–432.
16 Lieuvin A, Labbe JC, Doree M, Job D. Intrinsic microtubule stability in interphase cells. *J Cell Biol* 1994; **124**:985–996.
17 Bacus SS, Gudkov AV, Lowe M, Lyass L, Yung Y, Komarov AP, *et al.* Taxol-induced apoptosis depends on MAP kinase pathways (ERK and p38) and is independent of p53. *Oncogene* 2001; **20**:147–155.
18 Ren Y, Jiang H, Yang F, Nakaso K, Feng J. Parkin protects dopaminergic neurons against microtubule-depolymerizing toxins by attenuating microtubule-associated protein kinase activation. *J Biol Chem* 2009; **284**:4009–4017.
19 Wittmann T, Hyman A, Desai A. The spindle: a dynamic assembly of microtubules and motors. *Nat Cell Biol* 2001; **3**:E28–E34.
20 Kaestner P, Bastians H. Mitotic drug targets. *J Cell Biochem* 2010; **111**:258–265.
21 Woods CM, Zhu J, McQueney PA, Bollag D, Lazarides E. Taxol-induced mitotic block triggers rapid onset of a p53-independent apoptotic pathway. *Mol Med* 1995; **1**:506–526.
22 Jordan MA, Wendell K, Gardiner S, Derry WB, Copp H, Wilson L. Mitotic block induced in HeLa cells by low concentrations of paclitaxel (Taxol) results in abnormal mitotic exit and apoptotic cell death. *Cancer Res* 1996; **56**:816–825.
23 Ye K, Zhou J, Landen JW, Bradbury EM, Joshi HC. Sustained activation of p34(cdc2) is required for noscapine-induced apoptosis. *J Biol Chem* 2001; **276**:46697–46700.
24 Rieder CL, Cole R. Microtubule disassembly delays the G2-M transition in vertebrates. *Curr Biol* 2000; **10**:1067–1070.
25 Coffey ET, Hongisto V, Dickens M, Davis RJ, Courtney MJ. Dual roles for c-Jun N-terminal kinase in developmental and stress responses in cerebellar granule neurons. *J Neurosci* 2000; **20**:7602–7613.
26 Chang L, Jones Y, Ellisman MH, Goldstein LS, Karin M. JNK1 is required for maintenance of neuronal microtubules and controls phosphorylation of microtubule-associated proteins. *Dev Cell* 2003; **4**:521–533.
27 Bjorkblom B, Ostman N, Hongisto V, Komarovski V, Filen JJ, Nyman TA, *et al.* Constitutively active cytoplasmic c-Jun N-terminal kinase 1 is a dominant regulator of dendritic architecture: role of microtubule-associated protein 2 as an effector. *J Neurosci* 2005; **25**:6350–6361.
28 Kawauchi T, Chihama K, Nabeshima Y, Hoshino M. The in vivo roles of STEF/Tiam1, Rac1 and JNK in cortical neuronal migration. *EMBO J* 2003; **22**:4190–4201.
29 Daire V, Giustiniani J, Leroy-Gori I, Quesnoit M, Drevensek S, Dimitrov A, *et al.* Kinesin-1 regulates microtubule dynamics via a c-Jun N-terminal kinase-dependent mechanism. *J Biol Chem* 2009; **284**:31992–32001.
30 Morfini G, Pigino G, Szebenyi G, You Y, Pollema S, Brady ST. JNK mediates pathogenic effects of polyglutamine-expanded androgen receptor on fast axonal transport. *Nat Neurosci* 2006; **9**:907–916.
31 Morfini GA, You YM, Pollema SL, Kaminska A, Liu K, Yoshioka K, *et al.* Pathogenic huntingtin inhibits fast axonal transport by activating JNK3 and phosphorylating kinesin. *Nat Neurosci* 2009; **12**:864–871.
32 Buee-Scherrer V, Goedert M. Phosphorylation of microtubule-associated protein tau by stress-activated protein kinases in intact cells. *FEBS Lett* 2002; **515**:151–154.
33 Liu F, Li B, Tung EJ, Grundke-Iqbal I, Iqbal K, Gong CX. Site-specific effects of tau phosphorylation on its microtubule assembly activity and self-aggregation. *Eur J Neurosci* 2007; **26**:3429–3436.
34 Tang SC. Predictive markers of tubulin-targeting agents in breast cancer. *Clin Breast Cancer* 2008; **8 (Suppl 2):**S79–S84.
35 Teraishi F, Wu S, Sasaki J, Zhang L, Davis JJ, Guo W, *et al.* JNK1-dependent antimitotic activity of thiazolidin compounds in human non-small-cell lung and colon cancer cells. *Cell Mol Life Sci* 2005; **62**:2382–2389.
36 Cuadrado A, Garcia-Fernandez LF, Gonzalez L, Suarez Y, Losada A, Alcaide V, *et al.* Aplidin induces apoptosis in human cancer cells via glutathione depletion and sustained activation of the epidermal growth factor receptor, Src, JNK, and p38 MAPK. *J Biol Chem* 2003; **278**: 241–250.
37 Mandlekar S, Yu R, Tan TH, Kong AN. Activation of caspase-3 and c-Jun NH2-terminal kinase-1 signaling pathways in tamoxifen-induced apoptosis of human breast cancer cells. *Cancer Res* 2000; **60**: 5995–6000.
38 Powers CJ, McLeskey SW, Wellstein A. Fibroblast growth factors, their receptors and signaling. *Endocr Relat Cancer* 2000; **7**: 165–197.